Shining ALP dark radiation

Joerg Jaeckel[1] and Wen Yin[2]

[1]*Institut für theoretische Physik, Universität Heidelberg, Philosophenweg 16, 69120 Heidelberg, Germany*
[2]*Department of Physics, Tohoku University, Sendai, Miyagi 980-8578, Japan*

(Received 1 December 2021; accepted 13 May 2022; published 2 June 2022)

String scenarios typically not only predict axionlike particles (ALPs) but also significant amounts of ALP dark radiation originating from the decay of the inflaton or a more general modulus. In this paper, we study the decay of such nonthermally produced relativistic (but massive) ALPs to photons. If the ALPs are sufficiently highly energetic, contribute to $\Delta N_{\rm eff} \gtrsim \mathcal{O}(0.001)$, and have a mass $m_a \gtrsim$ MeV we find that, using observations of x-, and γ-rays, the CMB and BBN, very small values of the ALP-photon coupling, can be probed, corresponding to an origin of this coupling at the string (or even Planck) scale.

DOI: 10.1103/PhysRevD.105.115003

I. INTRODUCTION

In string or M theory, "axions" are ubiquitous, and one of them may even be the QCD axion [1–10]. In particular, it is likely that one or more of these axions couples to the standard model (SM) photon in M theory [5]. In the following, we will focus on such "axions" coupled to two-photons but heavier than the QCD axion. To make this distinction explicit, we will refer to them as axionlike particles (ALPs). (For some reviews of axions or ALPs, see [11–17].) The masses of such ALPs are generated by nonperturbative effects and therefore, are expected to feature a logarithmic scaling [2–5,7,18,19].[1] They can be either heavy or light but are unlikely to be massless since quantum gravity is argued to break any global symmetry, e.g., [21–30][2] (for a nice introduction of the string landscape see, e.g., [31]).

In the early Universe, it is plausible, perhaps even likely, that reheating proceeds via the decay of a modulus, which can also be the inflaton itself. The superpartner of such a modulus may be the axionlike particle that we are interested in. Then, if kinematically allowed, the ALPs are naturally produced in the modulus' decays. Those ALPs contribute to the dark radiation. Such dark radiation ALPs are widely discussed as a cosmic axion background (CAB) [32–41].[3] Alternatively or even additionally, ALP dark radiation may arise from a relatively long-lived subdominant species that has a sizable branching fraction into ALPs. Tests of the CAB using ALP-photon conversion in Earth-based experiments were studied in [35,38,40]. In addition, ALP-photon conversion may occur in astrophysical and cosmological magnetic fields, leaving potentially detectable imprints [43–49].

ALPs may also be produced via thermal scattering if they couple to the standard model particles. This yields very strong cosmological bounds [50–58]. However, those are typically contingent on a sufficiently high reheating temperature or large ALP photon coupling such that the ALPs thermalize [55]. In contrast, the situation outlined above and focused on in the present paper is usually associated with rather low reheating temperatures or small ALP photon coupling such that the thermal bounds will often not apply.

In this paper, we carefully study a situation where the ALPs constituting ALP dark radiation (or ALP hot dark matter), produced from the decay of a precursor particle, themselves decay to photons.[4] We estimate carefully the dark radiation contribution to the deviation of the effective

[1]In Ref. [20], it was mentioned that the ALP mass in M theory [5] is sensitive to the running of the gauge couplings. Here, we note that the axion may be heavy in the gauge mediation scenario of supersymmetry breaking, in which case, the gauge coupling, $\alpha_{\rm GUT}$, is much stronger than $1/25$ at the string scale, and the ALP mass $\propto \exp[-2\pi/\alpha_{\rm GUT}]$ is significantly enhanced.

[2]Interestingly, a nonvanishing fraction of the early works [24–26] discusses axions.

[3]Indeed, the CAB has an even longer history. It was discussed already in 1989 that neutrinos from the cosmic neutrino background may decay into an ALP (or majoron) to produce the axion background [42]. The nonthermal ALP produced in this way decays into photons to generate distortions in the CMB.

[4]There are also several studies discussing the decays of heavy ALPs emitted from astrophysical objects, in particular supernovae, around the present Universe [59–62]. Recently, it was also suggested that decaying (or converting) ALPs may result from the evaporation of primordial black holes [63]. By carefully measuring the resulting photon spectrum, it may be possible to distinguish this scenario from ours.

number of neutrino, $\Delta N_{\rm eff}$, by taking account of the decoupling effect. If this is measured in the future by cosmic microwave background (CMB) and baryonic acoustic oscillation (BAO) experiments [64–66], it is a probe of the ALP radiation at the recombination epoch. Then, we study the ALP decays to photons by taking account of their mass. This requires sufficiently massive ALPs and therefore, complements the tests via conversion, which usually focus on sub-eV masses. For the mother particle decay, we consider both cases that the precursor particle decays before and after reheating, the latter of which includes the present period meaning that the mother particle is part of the dark matter (DM). We also discuss the possibility that the ALP radiation becomes nonrelativistic after the recombination; i.e., it constitutes a component of hot dark matter. We find that such decaying ALPs can be constrained and tested up to very large decay constants, even up to the string scale if the mass $m_a \gtrsim 1$ MeV. In this way, string or M theory may be tested via future x- and γ-ray observations by, e.g., ATHENA [67], CTA [68], eROSITA [69], Fermi-Lat [70,71], GAMMA-400 [72,73], XRISM [74], and the CMB spectra, in addition to the $\Delta N_{\rm eff}$ measurement.

II. REVIEW OF ALP RADIATION FROM THE DECAY OF HEAVY PARTICLES

Let us briefly recall the main features of the scenario we want to consider, mainly following [41], but similar setups can also be found in [36–38,40].

For concreteness, let us consider a modulus field, ϕ. Our discussion does not change if this modulus is replaced by any other heavy particle, such as an inflaton or a heavy gravitino, that has two-body decays into an ALP in the early stages of the Universe. In the following, unless otherwise stated and especially for the numerical estimates, we assume that ϕ at one point dominated the Universe and decays to reheat the Universe. Let us stress, however, that even if the mother particle does not dominate the Universe, the bounds we will derive do not change if we replace the reheating temperature, T_R, by the decay temperature, T_ϕ, with the same definition, given below in Eq. (3). The mother particle may be produced thermally, nonthermally including gravitationally, by misalignment [75–77], or via other particles decay etc. The only feature we make use of is that it is nonrelativistic at the time of decay, but even if this is not the case, we expect that qualitatively similar results can be obtained in many other situations.

The total ϕ decay rate to the standard model particles via higher dimensional terms can be given in the form of

$$\Gamma_\phi = \kappa \frac{m_\phi^3}{M^2}. \tag{1}$$

Here, m_ϕ is the modulus mass, and κ is a coefficient encoding the details of the decay. M is the scale of the higher dimensional term giving rise to the interaction, and it may be regarded as the cutoff scale of the theory. Allowing for two- or three-body phase space suppression, we expect $\kappa \sim \mathcal{O}(0.1) - \mathcal{O}(10^{-3})$. Typical moduli but also the gravitino usually behave in this manner with $M \sim M_{\rm pl}$.

Smaller values of κ may be motivated by requiring that the radiative corrections to the mass squared caused by the higher-dimensional interaction are smaller than m_ϕ^2, giving $\kappa \lesssim m_\phi^2/M^2$. This is the case if the mother particle is another ALP, which is stabilized in a CP-violating vacuum, decaying into the ALP or SM particles via mixing with daughter ALP or heavy modulus. Then the decay rate is suppressed by the mixing (see, e.g., Appendix A of [78]). Moreover, requiring that the coupling does not cause a too large (tree or radiative) correction to the Higgs mass squared $\kappa \lesssim (100\ {\rm GeV}/M)^2$ may be needed for large m_ϕ (see [79] for a more detailed discussion). This may be particularly important if the supersymmetry scale is as high as M. Those radiative correction arguments are usually used in the context that ϕ is the inflaton that needs a flat potential to satisfy the slow-roll conditions. Therefore, κ is model dependent.

The decay reheats the Universe with the reheating temperature defined by

$$T_R \equiv (g_\star \pi^2/90)^{-1/4} \sqrt{\Gamma_\phi M_{\rm pl}}. \tag{2}$$

This yields

$$T_R \approx 20\ {\rm MeV} \sqrt{\kappa} \left(\frac{M_{\rm pl}}{M}\right) \left(\frac{11}{g_\star}\right)^{1/4} \left(\frac{m_\phi}{100\ {\rm TeV}}\right)^{3/2}, \tag{3}$$

where we use $M_{\rm pl} \approx 2.4 \times 10^{18}$ GeV for the reduced Planck mass. As indicated by the benchmark values in the equation, such scenarios often have a quite low reheating temperature. The decay temperature, T_ϕ, when ϕ does not dominate the Universe, can be obtained analogously from $H = \Gamma_\phi$, where H is the Hubble parameter at the decay evaluated in a standard ΛCDM scenario.

Below, we will recall how to calculate the spectrum of the ALPs resulting from the ϕ decay in the case where it is dominating the energy density. This requires the density of ϕ as an input, but the initial density of radiation is not important. As described in [41], this can be obtained by solving the coupled Boltzmann equations for the density ρ_ϕ and the entropy density s_r, completed by expressions for the Hubble rate H, the temperature T, and the radiation energy density ρ_r,

$$\dot{\rho}_\phi + 3H\rho_\phi = -\Gamma_\phi \rho_\phi, \tag{4}$$

$$\dot{s}_r + 3H s_r = c[t] \Gamma_\phi \rho_\phi, \tag{5}$$

$$c[t] = \frac{4(T g'_{s\star} + 3 g_{s\star})}{3T(T g'_\star + 4 g_\star)}, \tag{6}$$

$$H \approx \sqrt{\frac{\rho_\phi + \rho_r}{3M_{\rm pl}^2}}, \tag{7}$$

$$T = \left(\frac{45}{2\pi^2 g_{s\star}} s_r\right)^{1/3}, \tag{8}$$

$$\rho_r = \frac{\pi^2 g_\star}{30} T^4, \tag{9}$$

where a prime denotes a derivative with respect to temperature. Here, the implicit assumption is that the thermalization of the SM plasma is much faster than the decay of ϕ and the expansion of the Universe. This should be valid in the reheating temperature range of our interest. The final inputs for our calculations are $g_\star$ and $g_{s\star}$, the relativistic degrees of freedoms of the energy density and the entropy density from [80].

The modulus naturally decays into ALPs that are kinematically available. In particular, it can couple to ALPs, a, via, e.g., [32–36,81,82],

$$\mathcal{L} \supset \frac{\phi}{F_a} \partial_\mu a \partial^\mu a, \tag{10}$$

where $1/F_a$ is the coupling between ϕ and a. A noteworthy case is that the modulus is the superpartner of the ALP, i.e., the saxion, or if it mixes with the saxion. Via this interaction the decay,

$$\phi \to aa, \tag{11}$$

is possible.

The decay rate of $\phi \to aa$ is given by [32–36,81,82]

$$\Gamma_{\phi\to aa} = \frac{1}{32\pi} \frac{m_\phi^3}{F_a^2}, \tag{12}$$

where we neglect the ALP mass m_a by assuming $m_\phi \gg m_a$. A component of the energy is transferred into the ALP if the branching fraction,

$$B_{\phi\to aa} \equiv \frac{\Gamma_{\phi\to aa}}{\Gamma_\phi}, \tag{13}$$

is nonvanishing. In the following, we assume that $B_{\phi\to aa} \ll 1$ (i.e. ALP production is not dominant) so that we can neglect its component in the expansion history of the Universe and satisfy the constraint on the expansion history around the BBN and recombination eras [83,84]. Note, however, that $B_{\phi\to aa} \sim 1$ is possible when ϕ does not dominate the Universe.

Such a component, if relativistic until the recombination epoch, contributes to the dark radiation as (cf., e.g., Refs. [32,33,35,79,85]),

$$\Delta N_{\rm eff} \sim 6.1 B_{\phi\to aa} \left(\frac{11}{g_{s\star}(T_R)^4 g_\star(T_R)^{-3}}\right)^{1/3}. \tag{14}$$

This can be derived analytically by assuming constant $g_\star, g_{s\star}$ during the ϕ decay. Again, we use the values of $g_{s\star,\star}$ given in [80] with the T_R definition (2) for the analytic estimation here and hereafter. On the other hand, the spectra and the bounds relevant to the x−, γ-ray observations will be obtained by solving the Boltzmann equation numerically given the temperature dependence of $g_{s\star,\star}$ in [80]. Note that, as long as the ALPs are sufficiently relativistic, $\Delta N_{\rm eff}$ does not depend on the mass or energy of the ALP. A more precise result, obtained by solving the relevant Boltzmann equations and integrating over the resulting ALP spectrum, is shown in Fig. 1. This demonstrates the good accuracy of the formula given above. That said, we have to be mindful of the effect of the decrease of $g_\star, g_{s\star}$ if we perform a precise analysis. The coefficient of Eq. (14), which is usually used in the literature, is not clearly defined when $g_\star, g_{s\star}$ change rapidly. This is obvious because it is then unclear which definition of $g_\star, g_{s\star}$ we should use in Eq. (14), despite $\Delta N_{\rm eff}$ (red points) being a smooth function. In fact, the entropy release can enhance $\Delta N_{\rm eff}$ above the naive estimate obtained by assuming a constant $g_\star, g_{s\star}$. This is because the thermalized radiation energy density scales as $\rho_r \propto s_r^{4/3} g_{s\star}^{-4/3} g_\star$. $\Delta N_{\rm eff} \propto \rho_a s_r^{-4/3} \sim Br_{\phi\to aa} \rho_r s_r^{-4/3} \propto g_{s\star}^{-4/3} g_\star$. We have used $\rho_a \sim Br_{\phi\to aa}\rho_r$, which is justified in such a short period that the expansion of Universe can be neglected. When $g_{s\star} \simeq g_\star$ decreases during the short period for ϕ decays, $\Delta N_{\rm eff}$ increases. This is also found in the figure by comparing the numerical and analytical results. In the case that ϕ does not dominate the Universe and decays much after BBN, the analytic estimation is good enough.

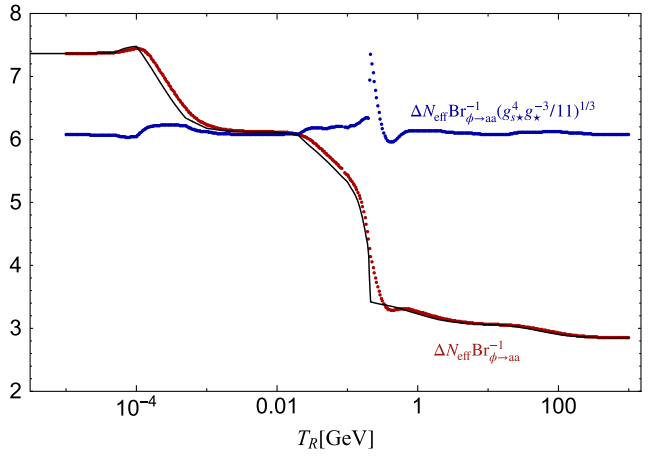

FIG. 1. Analytical (black solid line) and numerical (red points) results for $\Delta N_{\rm eff} B^{-1}_{\phi\to aa}$ by varying T_R and assuming that the relativistic a does not decay until the present. We also show $\Delta N_{\rm eff} B^{-1}_{\phi\to aa} (\frac{11}{g_{\star s}(T_R)^4 g_\star(T_R)^{-3}})^{-1/3}$ (blue points) for easy comparison with Eq. (14).

It is noteworthy that ALPs contributing to $\Delta N_{\rm eff} > \mathcal{O}(0.01)$ at around the recombination era can be measured in future CMB and BAO experiments [64–66].

The log-differential energy density of a with momentum p_a at t is given by (see, again, [41] for details but note that here we use a log-energy differential distribution)

$$\rho_{a,p_a}[t] \equiv \frac{p_a^3\sqrt{p_a^2+m_a^2}}{2\pi^2} f_{a,p_a}[t] \tag{15}$$

$$= 16E_a^4 \frac{\Gamma_{\phi\to aa}\rho_\phi(t')}{H(t')m_\phi^4}\theta(t-t'), \tag{16}$$

where $f_{a,k}$ is the distribution function of a, $E_a = \sqrt{p_a^2+m_a^2}$ is the energy of a, and we have neglected m_a in the last line. t' is related with t by $R[t']m_\phi/2 = R[t]p_a$ (cf., [41]), where R denotes the scale factor related to the redshift, z, via $1+z = 1/R$. Note that this log-differential distribution is defined such that the total ALP energy density is given by $\rho_a = \int \rho_{a,p_a} d\log p_a$. The form of the distribution function can be derived from the Boltzmann equation (see [41]),

$$\dot{f}_{a,p_a} = H\vec{p}_a \frac{\partial f_{a,p_a}}{\partial \vec{p}_a} + C^{(\rm coll)}_{p_a}, \tag{17}$$

$$C^{(\rm coll)}_{p_a} = 2n_\phi \Gamma_{\phi\to aa}\delta(p_a-\bar{m})\left(\frac{\bar{m}^2}{2\pi^2}\right)^{-1}, \tag{18}$$

$$\bar{m} \equiv \frac{1}{2}m_\phi\sqrt{1-\frac{4m_a^2}{m_\phi^2}}. \tag{19}$$

Here, the second row denotes the collision term for the mother particle decay by neglecting the Bose-enhancement effect. We can analytically obtain the solution of the distribution function to be

$$f_{a,p_a}[t] \approx \left.\frac{4\pi^2\Gamma_{\phi\to aa}n_\phi}{H\bar{m}^3}\right|_{t=t'} \tag{20}$$

by imposing the initial condition $f_{a,\vec{k}}[t\to-\infty] = 0$.

We will assume that the ALPs remain relativistic during the timescales of our interest. We also define $\hat{p}_a$ by $p_a = (1+z)\hat{p}_a$ for p_a at the redshift z. If it travels freely up to the present, the ALP today has a typical momentum of

$$p_a^{\rm peak} \simeq 2\times10^{-13}\ {\rm GeV}\frac{m_\phi}{g_{\star s}[T_R]^{1/3}T_R},$$

where $p_a^{\rm peak}$ corresponds to the momentum where $f_{a,p_a}[t\gg t']$ is maximal. The corresponding energy is

$$E_{\rm peak} \equiv \sqrt{(p_a^{\rm peak})^2+m_a^2}. \tag{21}$$

We stress that this is the typical energy that the ALP would have *today* if it did not decay.

For $M = M_{\rm pl}$ and $m_\phi = 100$ TeV and κ [defined in Eq. (1)] in the range 0.001–0.1, this formula gives $p_a^{\rm peak} \sim$ 1–10 keV.

Higher peak momenta can be achieved by lowering the reheating temperature. Note, however, for temperatures lower than about an MeV, the modulus cannot dominate the Universe in order to have successful BBN. One can also allow for larger m_ϕ. To realize this, while keeping T_R fixed, one needs to have very small values of κ (i.e., the modulus need to be in some sense sequestered from the SM and the axion and have no other decay channels; see also the discussion above). More generally, we can consider the case where the abundance of the original modulus is suppressed but potentially with a larger branching fraction to axions. The reheating temperature T_R is then replaced by the decay temperature T_ϕ. In this case, larger values of the peak momenta are possible without violating the observational constraints from reheating.

To illustrate the range of achievable values, we show $p_a^{\rm peak}$ by varying the decay temperature, T_ϕ (which is obtained from the equation $H = \Gamma_\phi$ where we neglect the axion or modulus contribution in H), or the reheating temperature, T_R, in Fig. 2. We find that if the modulus decays after the recombination temperature ∼eV, we can have peak momenta above an MeV (blue lines). Moreover, if we consider a situation where radiative corrections need to be suppressed, e.g., if ϕ is the inflaton or if the supersymmetric scale is high, this will result in a larger $p_a^{\rm peak}$ for a given reheating or decay temperature (red lines).

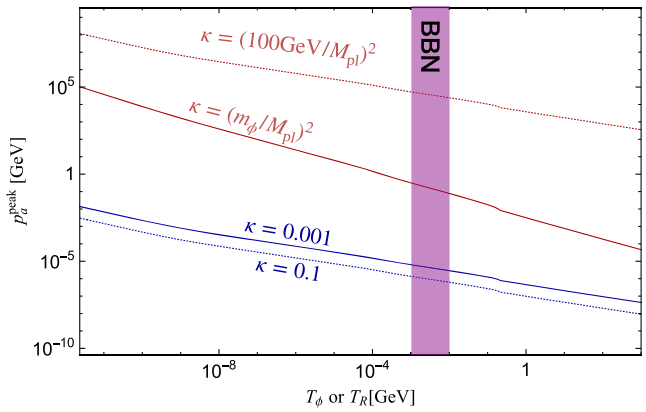

FIG. 2. Typical peak energy and decay or reheating temperature for different scenarios. Along the lines, we vary m_ϕ. Two fairly generic cases are $\kappa = 0.1$ (blue dashed line) and 0.001 (blue solid line) with $M = M_{\rm pl}$. We also show two cases where κ is suppressed (red lines). In the case m_ϕ^2 (weak scale^2), the respective scale is stable under radiative correction of $O(M_{\rm pl})^2$.

We also indicate the lower bound of the reheating temperature (purple band), which is needed for the success of big-bang nucleosynthesis [86–97]. Note, however, that this constraint is alleviated if ϕ is subdominant and not responsible for the reheating of the Universe. Following this, we consider in the present paper rather large ranges of the ALP peak momentum. Results for a generic modulus of $\kappa = 0.001$–1 that is reheating the Universe are shown in Figs. 7 and 10. In addition, in Figs. 8 and 9, we also show the results with larger $p_a^{\rm peak}$ to take account of more general situations.

As already mentioned, some ALPs may couple to SM particles and, in particular, photons via

$$\mathcal{L} \supset \frac{g_{a\gamma\gamma}}{4} a F_{\mu\nu}\tilde{F}^{\mu\nu}, \tag{22}$$

where $F_{\mu\nu}$ ($\tilde{F}^{\mu\nu}$) is the field strength of the SM photon (its dual), and $g_{a\gamma\gamma}$ is the photon coupling. If the scattering rate between ALPs and plasma photons (or other weak bosons in the symmetric phase) is lower than the expansion rate, $C_{\rm th} g_{a\gamma\gamma}^2 T_R^3 \lesssim \sqrt{g_\star \pi^2/90} T_R^2/M_{\rm pl}$, i.e., (cf., also [55])

$$g_{a\gamma\gamma} \lesssim 10^{-9}\ {\rm GeV} \frac{0.01}{C_{\rm th}} \left(\frac{100\ {\rm GeV}}{T_R}\right)^{1/2}, \tag{23}$$

the ALP rarely interacts with the ambient plasma. Here, $C_{\rm th}$ is a model-coefficient depending on how a couples to gauge fields in the symmetric phase.

If light, such dark radiation ALPs have the potential to be detected via ALP-photon conversion [35,38,40,43–49]. However, in this paper, we will use the same coupling to study the decay of heavier ALPs. We will find that if $m_a > \mathcal{O}({\rm keV})$, the constraints can be stronger than any existing constraints. Future observations of such photons will provide a nice opportunity to search for the dark radiation and traces of reheating.

Also note that Eq. (23) delineates the opposite case of the thermal production that was used in [54,55]. In this sense, the bound obtained therein, and the ones we will derive complement each other.

III. DECAYING DARK RADIATION

Now let us focus on the decay of the ALP radiation. Including the Lorentz factor E_a/m_a, the ALP decays into the photon pair with an energy dependent width,

$$\Gamma_a[p_a] = \frac{g_{a\gamma\gamma}^2}{64\pi}\frac{m_a^4}{E_a}. \tag{24}$$

When $p_a \gg m_a$, we have,

$$\Gamma_a[p_a] \simeq \frac{g_{a\gamma\gamma}^2}{64\pi}\frac{m_a^4}{\hat{p}_a(1+z)}, \tag{25}$$

and for $p_a \ll m_a$, we have the usual,

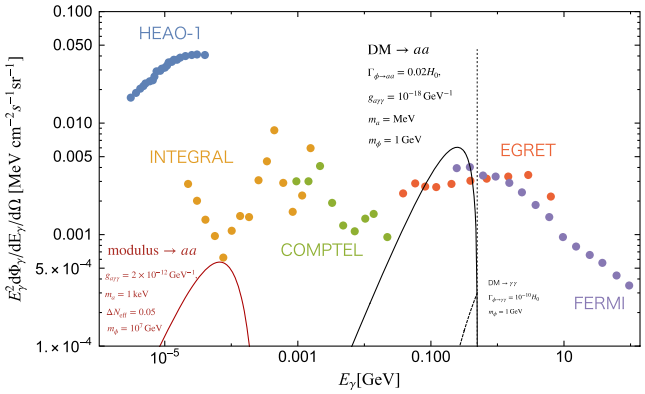

FIG. 3. The photon spectrum from the decay of ALP dark radiation itself originating from a modulus decay (red solid line) in the early Universe or from DM decay (black solid line). We take $g_{a\gamma\gamma} = 2\times10^{-12}\,{\rm GeV}^{-1}$, $m_a = 1$ keV, $m_\phi = 10^7$ GeV, $T_R = 10$ MeV, and $\Delta N_{\rm eff} = 0.05$ for case of relativistic ALPs from modulus decays. For the DM decay case, we take $\Gamma_{\phi\to aa} = 0.02 H_0$, $g_{a\gamma\gamma} = 10^{-18}\,{\rm GeV}^{-1}$, $m_a = {\rm MeV}$, with H_0 being the Hubble constant. For comparison, we also show the ordinary photon spectrum from direct DM decay with $\Gamma_{\phi\to aa} = 10^{-10} H_0$ and DM mass $m_\phi = 1$ GeV. The points indicate the photon flux observed from HEAO-1 [98], INTEGRAL [99], COMPTEL [100], EGRET [101], and FERMI [70] experiments. All of these are adopted from Ref. [102].

$$\Gamma_a[p_a] = \frac{g_{a\gamma\gamma}^2}{64\pi} m_a^3. \tag{26}$$

First, let us consider the decay of the ALP when it is relativistic. Then, we will discuss the possibility that the ALP radiation becomes nonrelativistic after recombination and decays into two photons. The photon energy density from the decay is obtained from the Boltzmann equation (see, e.g., [41]),

$$\dot{\rho}_{\gamma,k} - Hk\frac{\partial \rho_{\gamma,k}}{\partial k} + 4H\rho_{\gamma,k} = \int_{-\infty}^{\infty} d\,\log k' P[k,k']\Gamma_a[k']\rho_{a,k'}, \tag{27}$$

where $\rho_{\gamma,k}$ is defined by (15) [but not (16)] with a replaced by γ everywhere. The kernel,

$$P[k,k'] = 2(k/k')^2\theta(k'-k), \tag{28}$$

is obtained from the phase space distribution of a two-body decay to massless modes and again we assumed $E_a \gg m_a$. An example photon spectrum is shown as the red solid line in Fig. 3.[5] We also display observed photon data, more

[5]We note that the spectrum is not cut off by the opacity of the Universe to photons in the early Universe. This is because the photons result from decays that happen later. This is in contrast to the decaying DM to photons, whose spectrum is cut off around values of the optical depth $\tau[\frac{m_\phi}{2E_\gamma}, E_\gamma] \sim 1$.

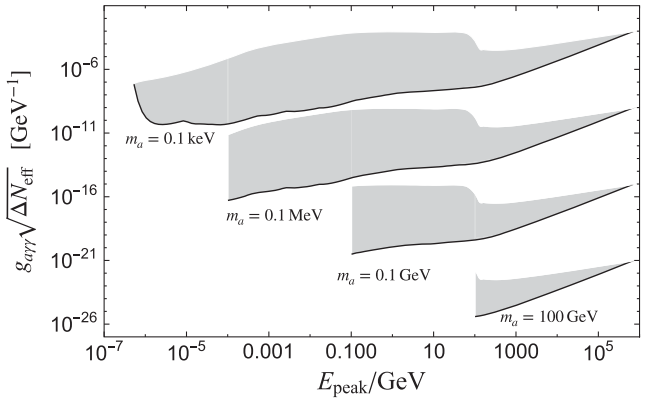

FIG. 4. The dark radiation bounds from x- and γ-ray observations [70,98–102] are shown in the $E_{\rm peak} - g_{a\gamma\gamma}\sqrt{\Delta N_{\rm eff}}$ plane. From top to bottom, the ALP mass is taken to be $m_a = 0.1$ keV, 0.1 MeV, 0.1 GeV, 0.1 TeV. We take $\Delta N_{\rm eff} = 0.1$. If we decrease $\Delta N_{\rm eff}$, the upper boundaries of the exclusions move down by $\sqrt{\Delta N_{\rm eff}}$, but the lower boundaries do not change.

precisely the 1σ upper bounds from HEAO-1 [98], INTEGRAL [99], COMPTEL [100], EGRET [101], and FERMI [70], which are adopted from [102]. The black solid line represents the photon spectrum from the cascade decay of the ALP originating from a decaying DM, which we will discuss in detail later (see Sec. IV).

One can see that x- and γ-ray observations set stringent bounds on the photon spectrum from the decay of the ALP dark radiation. Requiring that the photon flux is below the data points, we obtain the bounds shown in Fig. 4 in the $E_{\rm peak} - g_{a\gamma\gamma}\sqrt{\Delta N_{\rm eff}}$ plane. In the region with $E_{\rm peak} \simeq m_a$, the ALP is nonrelativistic (the region $E_{\rm peak} < m_a$ is kinematically forbidden). However, as we will see below, e.g., in Figs. 7, 8, 9, and 10, the nonrelativistic ALP (or hot dark matter) features a similar bound. The limit region also features an upper boundary. This is due to the early decay of the ALP radiation. If the decay were too early, the photon would not freely propagate to Earth and the x-, γ-ray bound is not applicable. This boundary is set by $e^{-\tau[z_{\rm dec}, E_{\rm peak}/2]} > 1/3$,[6] with $\tau[z_{\rm dec}, E_{\rm peak}]$ being the optical depth. Here, $z_{\rm dec}$ is the solution of $\Gamma[p_a] = 4H$. We adopt τ of the min-UV model from Ref. [103].

Photons from decays before recombination, on the other hand, are constrained by limits on the energy injection that would lead to distortions in the CMB and changes in BBN. A detailed simulation of this is beyond our scope. Here, we will instead recast the energy injection constraints from the CMB [104–110] and BBN [86–97] for the decay of nonrelativistic heavy particles, which is well studied. To this end, let us compare the photon energy from decaying ALP DM and decaying ALP radiation. In both cases of a nonrelativistic and a relativistic a decay, the total energy deposition around the time t is given by integrating the (logarithmic) energy spectrum of the ALPs multiplied by the fraction $\Gamma_a dt$ that decays during a given time interval dt. This results in

$$\Delta\rho_\gamma \propto dt \int \rho_{a,k}\Gamma_a[k] d\,\log\,k \tag{29}$$

$$\sim \rho_a \frac{\Gamma_a[E_{\rm peak}]}{H} d\,\log\,(1+z). \tag{30}$$

In the second line, we have roughly approximated the momentum integral by assuming that the (average) decay rate is given by the value at the peak momentum of the spectrum for illustrative purposes. Moreover, we have replaced the time integral by one over redshift.

Neglecting changes in the comoving ALP number, i.e., assuming that only a small fraction of ALPs decay, we have in both cases,

$$\Gamma_a \rho_a \propto R^{-3}, \tag{31}$$

since the dark radiation (matter) has $\rho_a \propto R^{-4}(R^{-3})$ and $\Gamma_a \propto R(R^0)$, respectively. This scaling also holds for the ALP radiation in Eq. (29) before the approximation. Therefore, as long as the comoving particle number does not change, we can reuse the known results for the nonrelativistic case to estimate the energy deposition at t. Indeed, we can use the same formulas by replacing the "lifetime" and the energy density at any fixed cosmic time, $\hat{t}$, via

$$\tau_a^{\text{non-rela}} \to \tau_a^{\rm rela} = 1/\Gamma_a[E_{\rm peak}[\hat{t}]], \tag{32}$$

and

$$\rho_a^{\text{non-rela}} \to \hat{\rho}_a^{\rm rela}[E_{\rm peak}[\hat{t}]]. \tag{33}$$

The comoving particle number is approximately constant if $t \lesssim \tau_a$, where we have defined the decay time $\tau_a[E_{\rm peak}]$ via

$$\Gamma_a[E_{\rm peak}] = 4H[\tau_a]. \tag{34}$$

In our analysis, we take $\hat{t} = \tau_a$ to recast the bound given in Refs. [92] and [104] for BBN and CMB, respectively. On the other hand, when the (exponential) decrease of the comoving ALP number cannot be neglected at t, the energy deposit until t is different between relativistic and nonrelativistic cases. Therefore, if τ_a is around or smaller than the typical timescale for the recombination and reionization or BBN era, the energy deposits are different, and our analysis is not very accurate. On the other hand, if τ_a is

[6]Strictly speaking, complete suppression would require a much smaller value. However, due to the exponential dependence of τ and the ambiguity in the photon backgrounds, we can use the simplified criterion without changing things dramatically.

much larger than those scales, which is our focus, our analysis should be valid.

A similar constraint arises when the decaying ALP is nonrelativistic at present but is relativistic at the recombination era, i.e., $p_a^{\rm peak} \lesssim m_a \lesssim p_a^{\rm peak}/R_{\rm rec}$.[7] This bound is obtained by the following simple procedure. We assume that the ALP contributes to today's cold DM with density,

$$\rho_a^{\rm nr} = \frac{m_a}{p_a^{\rm peak}} \Delta N_{\rm eff} \frac{7}{4} \frac{\pi^2}{30} T_\nu^4, \tag{35}$$

with T_ν being the present neutrino temperature.

Then we can estimate the photon flux from the nonrelativistic ALP decays by the formula [see Eq. (16) and the comments below it],

$$E_\gamma^2 \frac{d^2\Phi_\gamma}{dE d\Omega} = 16 E_\gamma^4 \frac{\Gamma_{a\to\gamma\gamma}[p_a = 0]\rho_a^{\rm nr}}{4\pi H(t') R[t']^3 m_a^4}, \tag{36}$$

in the energy range of

$$p_a^{\rm peak}/2 \le E_\gamma \le m_a/2. \tag{37}$$

This photon spectrum looks like the black dotted line in Fig. 3 without the line peak. Being a bit more precise, the part of the spectrum $E_\gamma < p_a^{\rm peak}/2$ mostly comes from the era when the ALP peak momentum $p_a^{\rm peak}/R[t'] > m_a$, and thus, the ALP becomes relativistic and our estimate is invalid. The spectrum there, however, is suppressed, and we do not consider it. This bound as well as the CMB and BBN bounds[8] can constrain the dark radiation (or the redshifted nonrelativistic ALP) even if the peak momentum is smaller than the mass. In particular, they are important when the peak momentum is much smaller than a keV (e.g., Fig. 10), in which case we cannot use the limits from the relativistic ALP decays.

Our analysis for the nonrelativistic regime of the ALPs should only be taken as an order of magnitude estimate when $p_a^{\rm peak}/R_{\rm rec} \lesssim 2m_a$ in which case, the ALP velocity today is smaller than the escape velocity of the Milky Way Galaxy. Then, the spatial distribution may be nontrivial.[9] We expect when $p_a^{\rm peak}/R_{\rm rec} \gg 2m_a$, i.e., in most of the range shown in the figures, the derived constraint is reasonably accurate. Throughout the numerical analysis in this paper, we have also neglected the effect of the ALP number change due to its decays, which should modify the resulting photon spectrum when $\Delta N_{\rm eff}$ is small and m_a is large (see, e.g., Ref. [111]).

We also note that $\rho_a^{\rm nr}/\rho_{\rm DM} \simeq 0.05 \times \Delta N_{\rm eff} \frac{\rm MeV}{p_a^{\rm peak}} \frac{m_a}{1\ {\rm GeV}}$, which is smaller than $\mathcal{O}(1)\%$ in the whole parameter region shown in the figures. This implies that the bounds from limits on hot DM are not severe.

In any case, when $m_a \gtrsim$ keV and $\Delta N_{\rm eff}$ is not extremely suppressed, the bounds on ALP dark radiation from x- or γ-ray, CMB, and BBN can be more stringent than other existing bounds.

The x- and γ-ray bound (gray region) as well as the recast CMB (orange region) and BBN (blue region) bounds are shown in Figs. 5 and 6 in the $E_{\rm peak}$ and $g_{a\gamma\gamma}\sqrt{\Delta N_{\rm eff}}$ plane. In Fig. 5, we fix $\Delta N_{\rm eff} = 0.1$, and 0.001. Above the red solid line, the ALP decays before the recombination era. It therefore does not contribute a form of dark radiation (or hot dark matter) that can be measured in the future CMB and BAO experiments. As expected from the figures, as long as $\Delta N_{\rm eff} = \mathcal{O}(10^{-3} - 1)$, the limits are very similar. In Fig. 6, the lower limits as well as the BBN and CMB bounds start to change. In this case (i.e., below the red solid line), however, the amount of the dark radiation is so small that it is difficult to probe it in future CMB and BAO experiments. In the three figures, the lower boundary of $g_{a\gamma\gamma}$ should be accurate, but the upper boundaries of the BBN and CMB may be considered as an order of magnitude estimate as we have discussed previously.

In Figs. 7, 8, 9, and 10, the bounds are represented in the $m_a - \sqrt{N_{\rm eff}} g_{a\gamma\gamma}$ plane by fixing $p_a^{\rm peak} = 10$ keV, 1 MeV, 1 GeV, 0.1 keV, respectively. For comparison, we also show the constraint from the extra cooling of horizontal branch stars as the purple dashed line (adopted from Refs. [112,113]; see also Refs. [114–116]). This is the only bound strongly sensitive to $\Delta N_{\rm eff}$. In the figures, we take $\Delta N_{\rm eff} = 0.1$.

As mentioned, our constraint does not change much if the ALP radiation is produced from a decaying mother particle that does not reheat the Universe. In the case of a two-body decay, the spectra of the ALP radiation only differ by a little [35,41]. However, the tiny difference of the ALP spectrum implies that we can possibly measure the reheating through it [41]. This is one of the reasons that we separated the two regions of relativistic ALP (solid line) and nonrelativistic ALP (dashed line). They do not have a significant difference for the purpose of limiting the parameter region of the models. However, they are different in future measurements; i.e., the photon spectra from the former carries the information of the mother particle, and the expansion history around ϕ decay [41], which is much harder to extract from the latter.

[7] As we mentioned, the case $p_a^{\rm peak}/R_{\rm rec} < m_a$, where the ALP is cold or warm dark matter, is not our focus, although the region can also be constrained. The bounds in the cold or warm dark matter regime can be found in various studies [86–97,104–110]. The difference between the ALP radiation and hot dark matter is not only the spectrum but also the contribution to $\Delta N_{\rm eff}$, which is measurable in the future CMB and BAO experiments.

[8] $p_a^{\rm peak}/R_{\rm rec} >$ several keVs is needed to apply and recast the CMB bound.

[9] In the case that the ALP is lighter than the inequality by a factor of a few, we may have an observational anisotropy of the x-, γ-rays in particular in the direction of galaxy clusters, which have larger escape velocity than the Milky Way Galaxy.

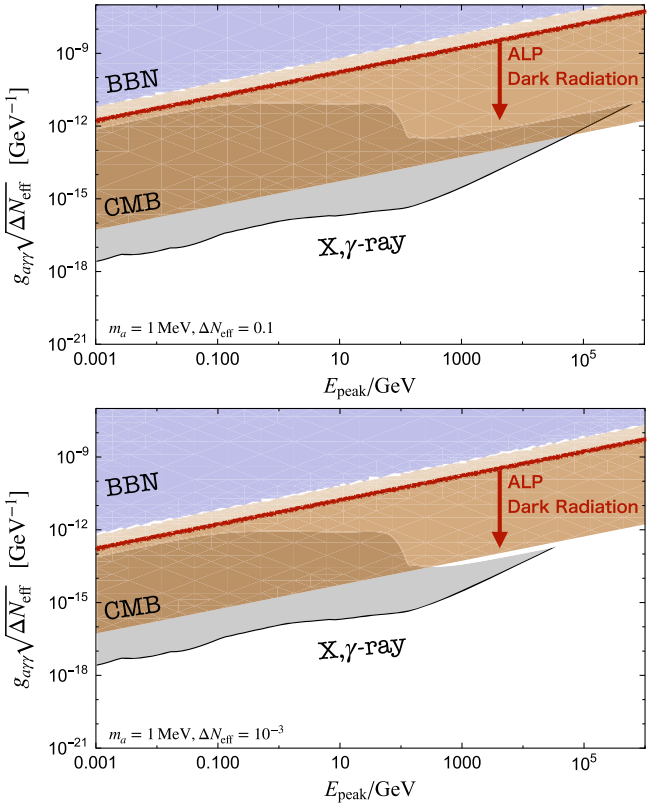

FIG. 5. The constraints for ALP dark radiation with $m_a = 1$ MeV, in the peak energy, $E_{\rm peak}$ and $g_{a\gamma\gamma}\sqrt{\Delta N_{\rm eff}}$ plane. with $\Delta N_{\rm eff} = 10^{-1}$ (upper one) and 10^{-3} (lower one). The blue, orange, and gray regions are excluded by the bounds from BBN, CMB, and x-,γ-ray observations, respectively, from top to bottom. Here, we fix $\Delta N_{\rm eff} = 0.1$, but the lower boundaries of the constraints do not change by varying $\Delta N_{\rm eff} = \mathcal{O}(10^{-3} - 1)$. We have adapted the BBN and CMB bounds from Ref. [92] and Ref. [104], respectively. As above the x-, γ-ray limits are from [70,98–102]. The optical depth is adopted from [103]. Below the red solid line, which is our main focus, the ALP dark radiation is present during the recombination epoch.

IV. CASCADE PHOTONS FROM DM DECAYING TO ALPs

So far, we have studied the situation where the dark radiation ALPs originate from the decay of a nonrelativistic modulus in the very early Universe. Our results showed that measuring x, γ-ray and CMB and BAO data have the opportunity in detecting the dark radiation from relatively heavy ALPs, which could even have a decay constant of the order of the string scale. In particular, when the ALP is relativstic until today, the resulting spectrum can carry the information of the expansion history in the early Universe and probably probe the reheating phase [41]. In the context to discriminate this reheating spectrum, let us consider a scenario that is not mentioned in [41] by using the model of the present paper. Concretely, let us study a situation where the ϕ decay happens much later and does not complete until

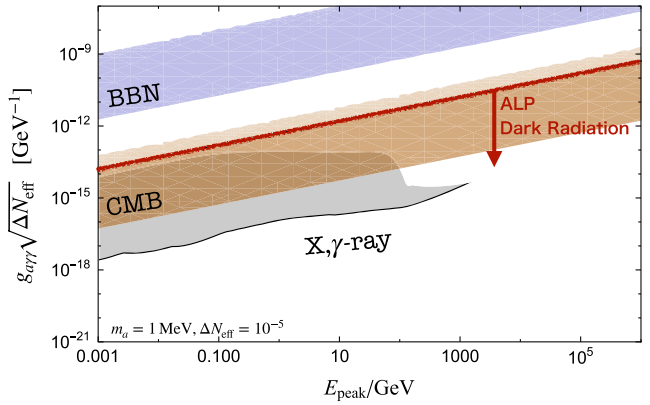

FIG. 6. Same as Fig. 5, but $\Delta N_{\rm eff}$ is taken to be 10^{-5} from which on the CMB and BBN bounds as well as the x-, γ-ray bound starts to change, significantly.

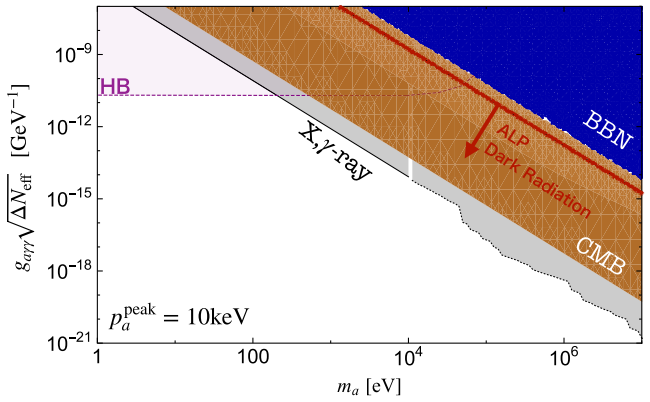

FIG. 7. Same constraints as Fig. 5 but in the $m_a - \sqrt{\Delta N_{\rm eff}} g_{a\gamma\gamma}$ plane and fixing $p_a^{\rm peak} = 10$ keV. $\Delta N_{\rm eff} = 0.1$ is taken. The cooling constraint from horizontal branch stars [112–116] is shown by the purple dashed line adopted from Ref. [112,113]. The constraints from photons when the ALP is nonrelativistic today is shown by the black dotted line by taking only the extragalactic component into account. By decreasing $\Delta N_{\rm eff}$, the purple dashed line moves downward, but other lower boundaries of the bounds do not change much for $\Delta N_{\rm eff} > 10^{-3}$.

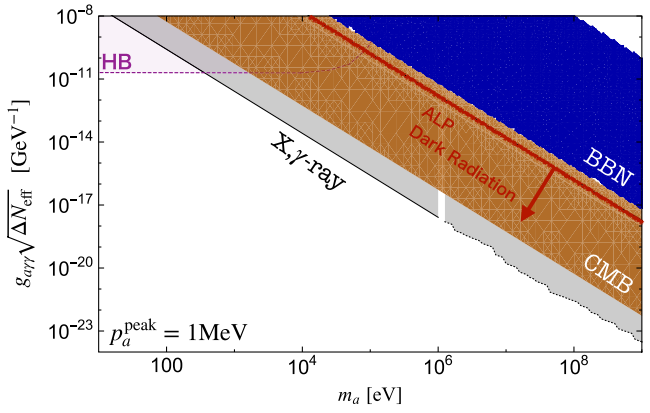

FIG. 8. Same as Fig. 7 with $p_a^{\rm peak} = 1$ MeV.

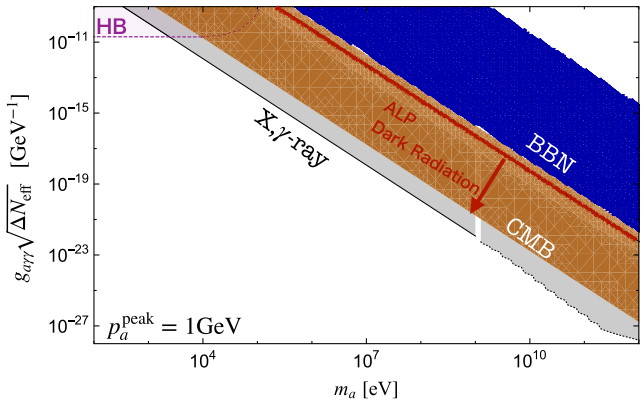

FIG. 9. Same as Fig. 7 with $p_a^{\rm peak} = 1$ GeV.

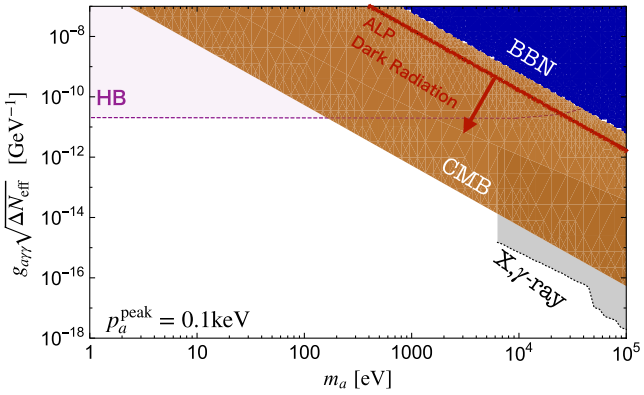

FIG. 10. Same as Fig. 7 with $p_a^{\rm peak} = 0.1$ keV. Since the peak energy is low, the x-, γ-ray constraint are only efficient when the ALP is heavy and becomes nonrelativistic until the present.

the present. We will see that this case can be probed as well, but the resulting γ (a) spectrum is (very) different.

Let us assume that the mother particle ϕ becomes nonrelativistic much before matter-radiation equality but decays after this time.[10] Then their spatial distribution is affected by structure formation, as they essentially behave like a fraction of the DM. In particular, ϕ will also be more concentrated in regions of high DM density such as the Galactic Center. In this situation, it is clear that we have a nontrivial spatial distribution. However, due to redshifting, galactic and extragalactic components will also have different spectra.

We start by considering the galactic and extragalactic components of the ALP spectrum and then discuss the corresponding photon spectra,

$$\rho_{a,E_a} = \rho_{a,E_a}^{\rm extra} + \rho_{a,E_a}^{\rm galactic}. \tag{38}$$

[10]A scenario in this spirit with DM particles decaying into axions (plus photons) has, e.g., recently been discussed in [117,118], albeit for lower axion and ALP mass.

As already noted, the angular distributions of the components are different. Clearly, the ALPs from the galactic component mostly come from the Galactic Center.

A. Extra galactic component

The discussion of the previous sections can be straightforwardly applied to the extragalactic component from Eq. (15) with $\rho_\phi \propto R^{-3}$, i.e.,

$$\rho_{a,E_a} \propto E_a \frac{\rho_c \Omega_\phi \Gamma_{\phi\to aa} \Theta[m_\phi/2 - E_a]}{H|_{z=m_\phi/2E_a-1}} \tag{39}$$

where ρ_c is the critical density, Ω_ϕ is the abundance of ϕ today, and we neglect the decrease in the comoving number of ϕ. In the dark energy dominated Universe, $\rho_{a,E_a} \propto E_a$, and it has a sharp cutoff at $E_a = m_\phi/2$. We can solve (27) to obtain the photon spectrum due to the ALP decay. The phase space suppression leads to the decrease of the spectrum with $\rho_{\gamma,E_\gamma} \propto |m_\phi/2 - E_\gamma|$ when $E_\gamma \sim m_\phi/2$. On the other hand, when $E_\gamma \ll m_\phi/2$, the spectrum is similar to the moduli decay case at lower energy (neglecting the difference of z dependence in H). Around the energy where the phase space is suppressed, the effect of the redshift is neglected. Then the photon energy is peaked at around $m_\phi/4$ since it is from the decay of ALP with $E_a = m_\phi/2$. The behavior agrees well with the numerical result presented in Fig. 3 with $\Omega_\phi h^2 = 0.12$. The extra galactic component is dominant compared to the galactic component if the ALP decay lifetime is not too short as we will see next.

B. Galactic component

Due to the gravitational interaction, a fraction of the nonrelativistic ϕ gathers around the Galactic Center. Since the distance from the Galactic Center is short, the redshift of the energies can be neglected. Then the ALP flux has an energy $m_\phi/2$, which is represented by

$$\frac{d\Phi_a^{\rm galactic}}{dE_a} = \int ds d\Omega \frac{\Gamma_{\phi\to aa}}{4\pi s^2} \left(\frac{\rho_\phi(s,\Omega)}{m_\phi}\right) s^2 \frac{dN_a}{dE}, \tag{40}$$

where s is the direction from the Sun along the line of sight, and Ω is the angular direction. Moreover, we have

$$\frac{dN_a}{dE} = 2\delta\left(E - \frac{m_\phi}{2}\right). \tag{41}$$

We can now use the D factor usually defined for decaying DM (cf., e.g., [119]),

$$D[\Omega] \equiv \int_{\Delta\Omega} d\Omega ds \rho_{\rm DM}(s,\Omega), \tag{42}$$

where $\Delta\Omega$ is the spatial angle covered by the object or region we are looking at. Combining this with the assumption,

$$\rho_\phi(s,\Omega) \approx \rho_{\rm DM}(s,\Omega)\frac{\Omega_\phi}{\Omega_{\rm DM}}, \tag{43}$$

i.e., ρ_ϕ has a distribution similar to that of DM, $\rho_{\rm DM}$, we can then calculate the ALP flux in a given direction,

$$\frac{d^2\Phi_a^{\rm galactic}}{dE_a d\Omega} = \frac{D(\Omega)}{\Delta\Omega}\frac{\Gamma_{\phi\to aa}}{(2\pi)m_\phi}\delta\left(E-\frac{m_\phi}{2}\right). \tag{44}$$

Depending on the angular direction, the ALP flux from the decaying DM may have a dominant contribution of galactic origin. The resulting ALP spectrum is same as the photon spectrum of the dashed line shown in Fig. 3, where the peak represents the ALP flux from the direction toward the center of galaxy. We take $m_\phi = 1$ GeV and $\Gamma_\phi = 10^{-10}H_0$. We assume the EinastoB distribution given in [103] for illustrative purpose.[11] One can see that the peak height is larger than that of the extragalactic component.

So far, this is identical to the case of an ordinary two-body decay of DM, e.g., into photons. However, up to now, we have only considered the ALP spectrum, but our observables are the photons from a subsequent decay of the ALPs. As we will see momentarily, this changes the situation significantly.

The photons from the decay of a relativistic ALP of energy E have the distribution of $dN_\gamma^{(a,E)}/dE_\gamma \simeq 2/E\Theta[E-E_\gamma]$ if we neglect the mass of a in the distribution. By noting that the photon is produced almost along the line of a-motion, the photon flux is approximated by

$$\begin{aligned}\frac{d\Phi_\gamma^{\rm galactic}}{dE_\gamma} &\approx \int_0^\infty ds d\Omega dE \frac{dN_\gamma^{(a,E)}}{dE_\gamma}(1-\exp(-s\cdot\Gamma_{a\to\gamma\gamma})) \\ &\quad\times\frac{\Gamma_{\phi\to aa}}{4\pi s^2}\left(\frac{\rho_\phi(s,\Omega)}{m_\phi}\right)s^2\frac{dN_a}{dE} \qquad (45)\\ &\approx 8\Gamma_{a\to\gamma\gamma}\frac{\Gamma_{\phi\to aa}}{4\pi m_\phi^2}\Theta[m_\phi/2-E_\gamma]\int_0^\infty ds d\Omega s\rho_\phi(s,\Omega), \qquad (46)\end{aligned}$$

where in the last line, we have assumed that the decay rate is small compared to the distance. Compared to Eq. (40), we have an additional factor of s in the integrand.

If a DM structure is localized around a given distance d from us, we can approximate

$$\int_{\Delta\Omega} ds d\Omega s\rho_\phi(s,\Omega) \sim d\times D[\Omega]. \tag{47}$$

Therefore, this component is important when the D factor and the distance d is large.

By integrating the EinastoB distribution for the Milky Way, the energy flux is peaked at $\sim 5\times10^{-6}\,{\rm MeV\,cm^{-2}\,s^{-1}\,sr^{-1}}$ with the parameter set for the cascade-decaying DM used in Fig. 3 (black solid line). We take $\Gamma_{\phi\to aa} = 2\times10^{-2}H_0$, $g_{a\gamma\gamma} = 10^{-18}$ GeV^{-1}, $m_\phi = 1$ GeV, $m_a =$ MeV. Therefore, the flux averaged by the angular integral is much smaller than the extra galactic component as can be expected from the suppression of the decay volume $r_\odot H_0$.

ALPs from far away galaxies can decay more efficiently due to the longer decay volume. Let us consider an $\mathcal{O}(100)$ Mpc distant cluster, e.g., the Ophiuchus galaxy cluster. We can then estimate [119],

$$E_\gamma^2\frac{d^2\Phi_\gamma^{\rm galactic}}{dE_\gamma d\Omega} \sim \mathcal{O}(10^{-4})\frac{\rm MeV}{\rm cm^2\ s\,sr}\frac{E_\gamma^2}{\rm GeV^2}\Theta(0.5\ {\rm GeV}-E_\gamma), \tag{48}$$

for the parameter set of the black solid line in Fig. 3. More precisely, we find the following estimated values for different example clusters: {0.0002 (A426), 0.00004 (Virgo), 0.00019 (Coma), 0.00023 (Ophiuchus), 0.00009 (A3526), 0.00011 (A3627), 0.00011 (AWM7), 0.00013 (A1367), 0.00023 (A3571), 0.00017 (A2199)}$\frac{\rm MeV}{\rm cm^2\ ssr}\frac{E_\gamma^2}{\rm GeV^2}\Theta(0.5\,{\rm GeV}-E_\gamma)$ for the galaxy cluster labeled in the bracket.

Although the galactic component of the ALP flux is comparable or a factor of a few larger than the extragalactic one, the photon flux is dominated by the extragalactic one, which is 2 orders of magnitude larger than the galactic component.

C. Discussion

Since the spectrum from the extragalactic component is similar to that of the moduli decay, we expect the lower bound from x-rays and γ-rays to be similar, with $\Delta N_{\rm eff}$ estimated by $\rho_{a,E}^{\rm extra}[z=\mathcal{O}(1)]$. We emphasize again that neglecting the galactic component in estimating the x-ray and γ-ray constraint is justified when the ALP radiation has a lifetime longer than the age of the Universe. When the lifetime of a is much shorter than the distance to the Galactic Center, the contribution from the galactic component can be more important than the extra galactic case.[12]

[11] We have estimated the height of the monochromatic peak by assuming an energy bin with width of $\Delta E/E = 0.01$.

[12] A generic cascade decay of DM with a suitable decay length for the ALP may be useful to explain nontrivial anisotropies in the distribution of cosmic-rays a la ultra-high energy cosmic rays above EeV, e.g., [120] (see, however, [121]), or something like the 3.5 keV line [122–126]. For example, if they are disfavored to originate from the Galactic Center of the Milky Way, a suitable decay length may lead to a relative brightening of objects at a distance of the order of the decay length.

Therefore the x-ray and γ-ray bound becomes even more stringent if the lifetime of ALP radiation is shorter than the timescale of recombination. This is different from the case of ALP radiation from the early Universe, which was our main topic.

Lastly, let us mention the possibility to distinguish between an early and a late decaying precursor particle, ϕ, from which the ALP is produced. When ϕ is the DM and decays late, the spectrum of the resulting photons is different from the early decay case, and thus, we can distinguish it if we have enough energy resolution (e.g., there are various experiments with energy resolution smaller or even much smaller than $\mathcal{O}(0.1)$ [67–74].) Another possible way to distinguish the two options is the angular distribution, which is more pronounced for the late decay case. While, as we have seen, individual structures are not exceptionally bright if the decay length is large, it may nevertheless be possible to pick them out, in particular, since they feature a slightly different energy spectrum. For example, let us look at the Galactic Center. Decay photons from there are not affected by redshift, and the peak of their spectrum is at $\sim m_\phi/4$. Therefore, this region of the spectrum should be slightly brighter when looking in the direction of the Galactic Center. This feature is absent if the ALP is produced from early moduli decay. In addition, in the case of late decay, $\Delta N_{\rm eff}$ measured by the CMB data is smaller than that for the decay to radiation around today, while the decaying dark radiation has same $\Delta N_{\rm eff}$ (or larger if the dark radiation mostly decays to the photon).

V. CONCLUSIONS

In this paper, we have calculated limits on ALP dark radiation, made from massive ALPs decaying into photons, from the observation of x- and γ-rays but also from recasting constraints on the energy injection during the CMB and BBN eras. We have focused on the case where the ALPs are produced in the decay of a heavy nonrelativistic precursor that could, e.g., be the inflaton or a modulus. In such, often string inspired, scenarios the reheating temperature is typically relatively low; thus, our limits complement those on thermally produced heavy ALPs [54,55].

It should be mentioned that our bounds depend on the peak energy of the ALP radiation spectrum. As discussed, this is model depend and hence is perhaps the main loophole to our analysis.

Keeping the just mentioned caveat in mind, if the mass is above MeV and $\Delta N_{\rm eff}$ is not too small, we can constrain photon couplings of the ALP originating from scales as high as the string or even Planck scale. In this sense, future observations of x- and γ-rays as well as the CMB provide an interesting opportunity to test ALPs with potentially stringy origin.

ACKNOWLEDGMENTS

J. J. would like to thank A. Hebecker and M. Wittner for discussions and collaboration on stringy setups with ALP dark radiation. W. Y. was supported by JSPS KAKENHI Grant Nos. 20H05851, 21K20364, 22K14029, and 22H01215.

[1] E. Witten, Phys. Lett. **149B**, 351 (1984).
[2] P. Svrcek and E. Witten, J. High Energy Phys. 06 (2006) 051.
[3] J. P. Conlon, J. High Energy Phys. 05 (2006) 078.
[4] A. Arvanitaki, S. Dimopoulos, S. Dubovsky, N. Kaloper, and J. March-Russell, Phys. Rev. D **81**, 123530 (2010).
[5] B. S. Acharya, K. Bobkov, and P. Kumar, J. High Energy Phys. 11 (2010) 105.
[6] T. Higaki and T. Kobayashi, Phys. Rev. D **84**, 045021 (2011).
[7] M. Cicoli, M. Goodsell, and A. Ringwald, J. High Energy Phys. 10 (2012) 146.
[8] M. Demirtas, C. Long, L. McAllister, and M. Stillman, J. High Energy Phys. 04 (2020) 138.
[9] V. M. Mehta, M. Demirtas, C. Long, D. J. E. Marsh, L. Mcallister, and M. J. Stott, arXiv:2011.08693.
[10] V. M. Mehta, M. Demirtas, C. Long, D. J. E. Marsh, L. McAllister, and M. J. Stott, J. Cosmol. Astropart. Phys. 07 (2021) 033.
[11] J. Jaeckel and A. Ringwald, Annu. Rev. Nucl. Part. Sci. **60**, 405 (2010).
[12] A. Ringwald, Phys. Dark Universe **1**, 116 (2012).
[13] P. Arias, D. Cadamuro, M. Goodsell, J. Jaeckel, J. Redondo, and A. Ringwald, J. Cosmol. Astropart. Phys. 06 (2012) 013.
[14] P. W. Graham, I. G. Irastorza, S. K. Lamoreaux, A. Lindner, and K. A. van Bibber, Annu. Rev. Nucl. Part. Sci. **65**, 485 (2015).
[15] D. J. E. Marsh, Phys. Rep. **643**, 1 (2016).
[16] I. G. Irastorza and J. Redondo, Prog. Part. Nucl. Phys. **102**, 89 (2018).
[17] L. Di Luzio, M. Giannotti, E. Nardi, and L. Visinelli, Phys. Rep. **870**, 1 (2020).
[18] T. Gherghetta, V. V. Khoze, A. Pomarol, and Y. Shirman, J. High Energy Phys. 03 (2020) 063.
[19] R. Kitano and W. Yin, J. High Energy Phys. 07 (2021) 078.
[20] D. J. E. Marsh and W. Yin, J. High Energy Phys. 01 (2021) 169.
[21] C. W. Misner and J. A. Wheeler, Ann. Phys. (N.Y.) **2**, 525 (1957).
[22] T. Banks and L. J. Dixon, Nucl. Phys. **B307**, 93 (1988).
[23] S. M. Barr and D. Seckel, Phys. Rev. D **46**, 539 (1992).
[24] M. Kamionkowski and J. March-Russell, Phys. Lett. B **282**, 137 (1992).

[25] R. Holman, S. D. H. Hsu, T. W. Kephart, E. W. Kolb, R. Watkins, and L. M. Widrow, Phys. Lett. B **282**, 132 (1992).
[26] R. Kallosh, A. D. Linde, D. A. Linde, and L. Susskind, Phys. Rev. D **52**, 912 (1995).
[27] T. Banks and N. Seiberg, Phys. Rev. D **83**, 084019 (2011).
[28] D. Harlow and H. Ooguri, Commun. Math. Phys. **383**, 1669 (2021).
[29] J. Alvey and M. Escudero, J. High Energy Phys. 01 (2021) 032.
[30] K. Yonekura, J. High Energy Phys. 09 (2021) 036.
[31] A. Hebecker, arXiv:2008.10625.
[32] M. Cicoli, J. P. Conlon, and F. Quevedo, Phys. Rev. D **87**, 043520 (2013).
[33] T. Higaki and F. Takahashi, J. High Energy Phys. 11 (2012) 125.
[34] S. Angus, J. P. Conlon, M. C. D. Marsh, A. J. Powell, and L. T. Witkowski, J. Cosmol. Astropart. Phys. 09 (2014) 026.
[35] J. P. Conlon and M. C. D. Marsh, J. High Energy Phys. 10 (2013) 214.
[36] A. Hebecker, P. Mangat, F. Rompineve, and L. T. Witkowski, J. High Energy Phys. 09 (2014) 140.
[37] C. Evoli, M. Leo, A. Mirizzi, and D. Montanino, J. Cosmol. Astropart. Phys. 05 (2016) 006.
[38] E. Armengaud *et al.* (IAXO Collaboration), J. Cosmol. Astropart. Phys. 06 (2019) 047.
[39] B. S. Acharya, M. Dhuria, D. Ghosh, A. Maharana, and F. Muia, J. Cosmol. Astropart. Phys. 11 (2019) 035.
[40] J. A. Dror, H. Murayama, and N. L. Rodd, Phys. Rev. D **103**, 115004 (2021).
[41] J. Jaeckel and W. Yin, Phys. Rev. D **103**, 115019 (2021).
[42] Z. G. Berezhiani, M. Y. Khlopov, and R. R. Khomeriki, Sov. J. Nucl. Phys. **52**, 65 (1990).
[43] T. Higaki, K. Nakayama, and F. Takahashi, J. Cosmol. Astropart. Phys. 09 (2013) 030.
[44] M. Fairbairn, Phys. Rev. D **89**, 064020 (2014).
[45] J. P. Conlon and M. C. D. Marsh, Phys. Rev. Lett. **111**, 151301 (2013).
[46] H. Tashiro, J. Silk, and D. J. E. Marsh, Phys. Rev. D **88**, 125024 (2013).
[47] A. Payez, C. Evoli, T. Fischer, M. Giannotti, A. Mirizzi, and A. Ringwald, J. Cosmol. Astropart. Phys. 02 (2015) 006.
[48] M. C. D. Marsh, H. R. Russell, A. C. Fabian, B. P. McNamara, P. Nulsen, and C. S. Reynolds, J. Cosmol. Astropart. Phys. 12 (2017) 036.
[49] C. S. Reynolds, M. C. D. Marsh, H. R. Russell, A. C. Fabian, R. Smith, F. Tombesi, and S. Veilleux, Astrophys. J. **890**, 59 (2020).
[50] M. S. Turner, Phys. Rev. Lett. **59**, 2489 (1987); **60**, 1101 (E) (1988).
[51] S. Chang and K. Choi, Phys. Lett. B **316**, 51 (1993).
[52] T. Moroi and H. Murayama, Phys. Lett. B **440**, 69 (1998).
[53] S. Hannestad, A. Mirizzi, and G. Raffelt, J. Cosmol. Astropart. Phys. 07 (2005) 002.
[54] D. Cadamuro and J. Redondo, J. Phys. Conf. Ser. **375**, 022002 (2012).
[55] D. Cadamuro and J. Redondo, J. Cosmol. Astropart. Phys. 02 (2012) 032.
[56] J. Jaeckel, J. Redondo, and A. Ringwald, Phys. Rev. D **89**, 103511 (2014).
[57] A. Salvio, A. Strumia, and W. Xue, J. Cosmol. Astropart. Phys. 01 (2014) 011.
[58] R. Daido, F. Takahashi, and W. Yin, J. High Energy Phys. 02 (2018) 104.
[59] M. Giannotti, L. D. Duffy, and R. Nita, J. Cosmol. Astropart. Phys. 01 (2011) 015.
[60] J. Jaeckel, P. C. Malta, and J. Redondo, Phys. Rev. D **98**, 055032 (2018).
[61] A. Caputo, P. Carenza, G. Lucente, E. Vitagliano, M. Giannotti, K. Kotake, T. Kuroda, and A. Mirizzi, Phys. Rev. Lett. **127**, 181102 (2021).
[62] F. Calore, P. Carenza, M. Giannotti, J. Jaeckel, G. Lucente, and A. Mirizzi, Phys. Rev. D **104**, 043016 (2021).
[63] F. Schiavone, D. Montanino, A. Mirizzi, and F. Capozzi, J. Cosmol. Astropart. Phys. 08 (2021) 063.
[64] A. Kogut *et al.*, J. Cosmol. Astropart. Phys. 07 (2011) 025.
[65] K. N. Abazajian *et al.* (CMB-S4 Collaboration), arXiv:1610.02743.
[66] D. Baumann, D. Green, and M. Zaldarriaga, J. Cosmol. Astropart. Phys. 11 (2017) 007.
[67] D. Barret *et al.*, Proc. SPIE Int. Soc. Opt. Eng. **10699**, 106991G (2018).
[68] M. Actis *et al.* (CTA Consortium Collaboration), Exper. Astron. **32**, 193 (2011).
[69] A. Merloni *et al.* (eROSITA Collaboration), arXiv:1209.3114.
[70] M. Ackermann *et al.* (Fermi-LAT Collaboration), Astrophys. J. **750**, 3 (2012).
[71] https://fermi.gsfc.nasa.gov.
[72] A. M. Galper *et al.*, Adv. Space Res. **51**, 297 (2013).
[73] A. E. Egorov, N. P. Topchiev, A. M. Galper, O. D. Dalkarov, A. A. Leonov, S. I. Suchkov, and Y. T. Yurkin, J. Cosmol. Astropart. Phys. 11 (2020) 049.
[74] XRISM Science Team, arXiv:2003.04962.
[75] J. Preskill, M. B. Wise, and F. Wilczek, Phys. Lett. **120B**, 127 (1983).
[76] L. Abbott and P. Sikivie, Phys. Lett. **120B**, 133 (1983).
[77] M. Dine and W. Fischler, Phys. Lett. **120B**, 137 (1983).
[78] D. Kim, Y. Kim, Y. K. Semertzidis, Y. C. Shin, and W. Yin, Phys. Rev. D **104**, 095010 (2021).
[79] J. Jaeckel and W. Yin, J. Cosmol. Astropart. Phys. 02 (2021) 044.
[80] L. Husdal, Galaxies **4**, 78 (2016).
[81] T. Higaki, K. Nakayama, and F. Takahashi, J. High Energy Phys. 07 (2013) 005.
[82] T. Moroi and W. Yin, J. High Energy Phys. 03 (2021) 301.
[83] N. Aghanim *et al.* (Planck Collaboration), Astron. Astrophys. **641**, A6 (2020); **652**, C4(E) (2021).
[84] B. D. Fields, K. A. Olive, T.-H. Yeh, and C. Young, J. Cosmol. Astropart. Phys. 03 (2020) 010; 11 (2020) E02.
[85] K. Choi, E. J. Chun, and J. E. Kim, Phys. Lett. B **403**, 209 (1997).
[86] M. Kawasaki, K. Kohri, and N. Sugiyama, Phys. Rev. Lett. **82**, 4168 (1999).
[87] M. Kawasaki, K. Kohri, and N. Sugiyama, Phys. Rev. D **62**, 023506 (2000).
[88] S. Hannestad, Phys. Rev. D **70**, 043506 (2004).

[89] K. Ichikawa, M. Kawasaki, and F. Takahashi, J. Cosmol. Astropart. Phys. 05 (2007) 007.
[90] F. De Bernardis, L. Pagano, and A. Melchiorri, Astropart. Phys. **30**, 192 (2008).
[91] P. F. de Salas, M. Lattanzi, G. Mangano, G. Miele, S. Pastor, and O. Pisanti, Phys. Rev. D **92**, 123534 (2015).
[92] M. Kawasaki, K. Kohri, T. Moroi, and Y. Takaesu, Phys. Rev. D **97**, 023502 (2018).
[93] M. Hufnagel, K. Schmidt-Hoberg, and S. Wild, J. Cosmol. Astropart. Phys. 11 (2018) 032.
[94] L. Forestell, D. E. Morrissey, and G. White, J. High Energy Phys. 01 (2019) 074.
[95] T. Hasegawa, N. Hiroshima, K. Kohri, R. S. L. Hansen, T. Tram, and S. Hannestad, J. Cosmol. Astropart. Phys. 12 (2019) 012.
[96] M. Kawasaki, K. Kohri, T. Moroi, K. Murai, and H. Murayama, J. Cosmol. Astropart. Phys. 12 (2020) 048.
[97] P. F. Depta, M. Hufnagel, and K. Schmidt-Hoberg, J. Cosmol. Astropart. Phys. 04 (2021) 011.
[98] D. E. Gruber, J. L. Matteson, L. E. Peterson, and G. V. Jung, Astrophys. J. **520**, 124 (1999).
[99] L. Bouchet, E. Jourdain, J. P. Roques, A. Strong, R. Diehl, F. Lebrun, and R. Terrier, Astrophys. J. **679**, 1315 (2008).
[100] S. C. Kappadath, *Measurement of the Cosmic Diffuse Gamma-Ray Spectrum from 800 keV to 30 MeV* (University of New Hampshire, Durham, 1998).
[101] A. W. Strong, I. V. Moskalenko, and O. Reimer, Astrophys. J. **613**, 962 (2004).
[102] R. Essig, E. Kuflik, S. D. McDermott, T. Volansky, and K. M. Zurek, J. High Energy Phys. 11 (2013) 193.
[103] M. Cirelli, G. Corcella, A. Hektor, G. Hutsi, M. Kadastik, P. Panci, M. Raidal, F. Sala, and A. Strumia, J. Cosmol. Astropart. Phys. 03 (2011) 051; 10 (2012) E01.
[104] V. Poulin, J. Lesgourgues, and P. D. Serpico, J. Cosmol. Astropart. Phys. 03 (2017) 043.
[105] J. R. Ellis, G. B. Gelmini, J. L. Lopez, D. V. Nanopoulos, and S. Sarkar, Nucl. Phys. **B373**, 399 (1992).
[106] W. Hu and J. Silk, Phys. Rev. Lett. **70**, 2661 (1993).
[107] J. A. Adams, S. Sarkar, and D. W. Sciama, Mon. Not. R. Astron. Soc. **301**, 210 (1998).
[108] X.-L. Chen and M. Kamionkowski, Phys. Rev. D **70**, 043502 (2004).
[109] T. Bringmann, F. Kahlhoefer, K. Schmidt-Hoberg, and P. Walia, Phys. Rev. D **98**, 023543 (2018).
[110] S. K. Acharya and R. Khatri, J. Cosmol. Astropart. Phys. 12 (2019) 046.
[111] S.-Y. Ho, F. Takahashi, and W. Yin, J. High Energy Phys. 04 (2019) 149.
[112] A. Ayala, I. Domínguez, M. Giannotti, A. Mirizzi, and O. Straniero, Phys. Rev. Lett. **113**, 191302 (2014).
[113] P. Carenza, O. Straniero, B. Döbrich, M. Giannotti, G. Lucente, and A. Mirizzi, Phys. Lett. B **809**, 135709 (2020).
[114] G. G. Raffelt, Phys. Rev. D **33**, 897 (1986).
[115] G. G. Raffelt and D. S. P. Dearborn, Phys. Rev. D **36**, 2211 (1987).
[116] G. Raffelt, *Stars as Laboratories for Fundamental Physics: The Astrophysics of Neutrinos, Axions, and Other Weakly Interacting Particles* (University of Chicago Press, Chicago, 1996).
[117] K. J. Bae, A. Kamada, and H. J. Kim, Phys. Rev. D **99**, 023511 (2019).
[118] Y. Gu, L. Wu, and B. Zhu, Phys. Rev. D **105**, 095008 (2022).
[119] C. Combet, D. Maurin, E. Nezri, E. Pointecouteau, J. A. Hinton, and R. White, Phys. Rev. D **85**, 063517 (2012).
[120] R. U. Abbasi *et al.* (Telescope Array), Astrophys. J. Lett. **790**, L21 (2014).
[121] R. U. Abbasi *et al.* (Telescope Array), Astrophys. J. Lett. **867**, L27 (2018).
[122] E. Bulbul, M. Markevitch, A. Foster, R. K. Smith, M. Loewenstein, and S. W. Randall, Astrophys. J. **789**, 13 (2014).
[123] O. Urban, N. Werner, S. W. Allen, A. Simionescu, J. S. Kaastra, and L. E. Strigari, Mon. Not. R. Astron. Soc. **451**, 2447 (2015).
[124] A. Boyarsky, J. Franse, D. Iakubovskyi, and O. Ruchayskiy, Phys. Rev. Lett. **115**, 161301 (2015).
[125] N. Cappelluti, E. Bulbul, A. Foster, P. Natarajan, M. C. Urry, M. W. Bautz, F. Civano, E. Miller, and R. K. Smith, Astrophys. J. **854**, 179 (2018).
[126] C. Dessert, N. L. Rodd, and B. R. Safdi, Science **367**, 1465 (2020).